

REPORT DOCUMENTATION PAGE

AFRL-SR-BL-TR-01-

he
ig

Public reporting burden for this collection of information is estimated to average 1 hour per response, including the time for reviewing instructions, data needed, and completing and reviewing this collection of information. Send comments regarding this burden estimate or any other a this burden to Department of Defense, Washington Headquarters Services, Directorate for Information Operations and Reports (0704-01 4302. Respondents should be aware that notwithstanding any other provision of law, no person shall be subject to any penalty for failing valid OMB control number. PLEASE DO NOT RETURN YOUR FORM TO THE ABOVE ADDRESS.

0381

1. REPORT DATE (DD-MM-YYYY) 12-25-2000		2. REPORT TYPE Final		3. DATES COVERED (From - To)	
4. TITLE AND SUBTITLE The Growth and Characterization of Ferrite-High Temperature Superconductor Thin Films for Microwave Devices				5a. CONTRACT NUMBER F49620-97-1-0235	5b. GRANT NUMBER
				5c. PROGRAM ELEMENT NUMBER	
6. AUTHOR(S) Kennedy, Robin J.				5d. PROJECT NUMBER	
				5e. TASK NUMBER	
				5f. WORK UNIT NUMBER	
7. PERFORMING ORGANIZATION NAME(S) AND ADDRESS(ES) Florida A&M University Department Of Physics Tallahassee Florida 32307				8. PERFORMING ORGANIZATION REPORT NUMBER RJK-PAS-0001	
9. SPONSORING / MONITORING AGENCY NAME(S) AND ADDRESS(ES) Air Force Office of Scientific Research Directorate of Physics & Electronics AFOSR/NE 801 N. Randolph St., Room 732 Arlington VA 22203-1977 USA				10. SPONSOR/MONITOR'S ACRONYM(S) Harold Weinstock , Ph.D., D.H.C.	
				11. SPONSOR/MONITOR'S REPORT NUMBER(S)	
12. DISTRIBUTION / AVAILABILITY STATEMENT DISTRIBUTION STATEMENT A Approved for Public Release Distribution Unlimited					
13. SUPPLEMENTARY NOTES Prepared in cooperation with Patricia A. Stampe					
14. ABSTRACT In an effort to integrate superconducting, conducting, ferrite and insulating thin films to produce microwave devices such as phase shifters and circulators, thin films (single and bi-layer) of ferrites (Strontium Hexaferrite, Fe_3O_4), superconductors ($YBa_2Cu_3O_{7-x}$), buffer layers (MgO), and ground planes ($SrRuO_3$, $CaRuO_3$) were grown by the technique of laser ablation on semiconducting (Si, GaAs), ferrite (YIG), and insulating ($LaAlO_3$) substrates. All films grown were epitaxial as shown by 4 circle x-ray diffractometry. The magnetic properties of the films were characterized by magnetometry and by FMR. 4 wire resistance measurements were used to characterize the superconducting properties.					
This investigation has shown that the development of suitable buffer layers is essential to stop chemical diffusion, reaction between the various compounds and to passivate the semiconducting substrates. The presence of multiple layers complicates matters, since epitaxy degrades with film thickness making some form of milling (ion beam) to preserve surface smoothness essential prior to deposition of succeeding layers.					
15. SUBJECT TERMS RADAR, Microwave Devices, Ferrite, Superconductor, Buffer layer, Ruthenate, Semiconductor, Epitaxial.					
16. SECURITY CLASSIFICATION OF: U			17. LIMITATION OF ABSTRACT UU	19a. NAME OF RESPONSIBLE PERSON 8 Robin J. Kennedy	
a. REPORT U			2 8	19b. TELEPHONE NUMBER (include area code) 850 599 8373	
b. ABSTRACT U			c. THIS PAGE U		



Florida A&M University

Tallahassee Florida 32307

Laser Ablation Facility
Rm. B326
National High Magnetic Field Lab.,
1800 Dirac Drive, Tallahassee, FL 32310

Ph. (850) 599 8373
FAX: (850) 599 8378

Harold Weinstock, Ph.D., D.H.C.
Air Force Office of Scientific Research
Directorate of Physics & Electronics
AFOSR/NE
801 N. Randolph St., Room 732
Arlington VA 22203-1977 USA

December 25, 2000

Dear Harold,

I enclose a copy of our final report for grant number F49620-97-1-0235 "The Growth and Characterization of Ferrite-High Temperature Superconductor Thin Films for Microwave Devices".

Sorry that it is so late.

Best Wishes

A handwritten signature in black ink, appearing to read "Robin Kennedy".

Robin Kennedy

FINAL REPORT

GRANT # F49620-97-1-0235

THE GROWTH AND CHARACTERIZATION OF FERRITE-HIGH TEMPERATURE SUPERCONDUCTOR THIN FILMS FOR MICROWAVE DEVICES

Program Manager: Dr. H. Weinstock, AFOSR

Principal Investigator: Dr. R.J. Kennedy
Florida A&M University
Tallahassee FL 32307

Co-PI: Dr. P.A. Stampe
Florida A&M University
Tallahassee FL 32307

Table of Contents

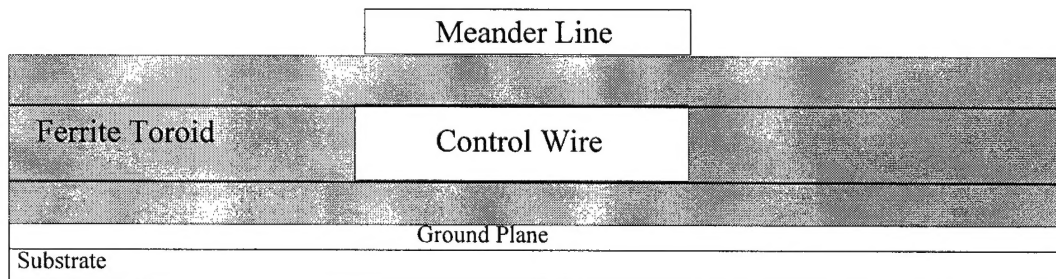
- 1. Objectives**
- 2. Experimental Procedure**
- 3. RESULTS: Growth and Characterization of Device Components**
 - 3.1 YBCO Films on Single Crystal YIG**
Growth of MgO Buffer Layers
 - 3.2 MgO Films on Single Crystal YIG**
 - 3.3 MgO Films on Polycrystalline YIG**
 - 3.4 Investigation of MgO Buffer Layer Growth on Various Substrates**
 - Growth of Superconductor on Buffered Ferrites*
 - 3.5 YBCO Films on MgO Buffered LaAlO₃**
 - 3.6 YBCO Films on MgO Buffered Single Crystal YIG**
 - Growth of Ferrites*
 - 3.7 Spinel Ferrite Films on Various Substrates**
 - 3.8 Strontium Hexaferrite Films**
 - Semiconductor Integration*
 - 3.9 YBCO Films on MgO Buffered Semiconductors**
 - Ground Plane Development*
 - 3.10 SrRuO₃ and CaRuO₃ Films on LaAlO₃**
 - 3.11 YBCO Films on CeO₂/YSZ/Ni**
- 4. Future Directions**
- 5. Students Employed**
- 6. Publications**
- 7. Summary**

1. Objective

The objective of the proposal was to integrate superconducting, conducting, ferrite and insulating thin films to produce microwave devices such as phase shifters and circulators. The phase shifter was to consist of a toroid of ferrite material in contact with a superconducting stripline (see sketch below). The ferrite toroid was to be switchable by means of a concentric control wire. The purpose of the control wire was to latch the ferrite into one or other of its magnetic remanent states. As a consequence, a phase shift would occur in the r.f. signal sent along the superconducting stripline. The toroid design was chosen since the deleterious effects of magnetic poles on the superconducting stripline are avoided. The complete device was to be made using thin film technology and was to be able to be integrated with semiconductor manufacturing.

To make the device would involve the deposition of several thin films as outlined in the following steps. The order of the steps could be reversed if it were beneficial.

1. Deposit a metallic ground plane
2. Deposition of the bottom layer of the toroid
3. By shadow masking or etching form the vertical walls of the toroid
4. Deposition of the first half layer of the central nonmagnetic spacer of the toroid
5. Deposit the control wire required for latching on top of the spacer layer
6. Deposit the second half of the spacer layer
7. Deposit the top layer of ferrite material to complete the toroid
8. Deposition of the superconducting meander line



Some simplification was anticipated. Since ferrite materials (YIG, Fe_3O_4 , etc) are highly resistive it is likely that the insulating spacer layer inside the toroid can be omitted and that the conducting control wire could act as the spacer layer. The control wire, like the superconducting meander line, could be made from $\text{YBa}_2\text{Cu}_3\text{O}_{7-x}$ (YBCO). Thus the complete device could be as simple as (1) ferrite bottom of toroid, (2) YBCO control line acting as a spacer, (3) ferrite top layer of toroid, (4) YBCO r.f. meander line. Some complications were anticipated to arise due to the chemical reactivity of the materials especially at their growth temperature (up to 750°) necessitating the inclusion of buffer layers between all deposited film layers.

Thus the project was expected to reduce to the growth of multilayers of ferrites, the growth of YBCO and possibly to the growth of buffer layers.

1.1 Choice of Materials

Ferrite: Yttrium Iron Garnet (YIG) was considered the optimal choice of ferrite material due to its proven application for microwave devices based upon its very narrow ferromagnetic resonance (FMR) linewidth. YIG is cubic, with a lattice parameter of 12.38Å. Other common microwave materials considered for this project were the various spinel ferrites (such as Fe_3O_4 based magnesium manganese ferrite and lithium ferrite) with cubic lattice parameters ranging from 8.2-8.5Å.

Conductor/Superconductor: $YBa_2Cu_3O_{7-x}$ was chosen as the superconducting meander line material (and as the control wire) since its superconducting temperature of approximately 90K is sufficiently higher than 77K to allow efficient operation at liquid nitrogen temperatures. Thin films of YBCO can be grown using laser ablation. These have excellent superconducting properties when deposited on perovskite substrates with similar lattice parameters to the YBCO, e.g. $LaAlO_3$, $SrTiO_3$, $BaTiO_3$. However, microwave ferrite materials have lattice parameters much larger than the in-plane lattice parameter of c-axis oriented YBCO (~3.85Å). Yttrium Iron Garnet has a cubic lattice parameter of 12.38 Å. In order to obtain high quality films of YBCO on these ferrites it is necessary to have a good lattice match with the underlying ferrite substrate. Although epitaxial growth is known to occur in some cases where a lattice match does not exist, it is generally necessary to grow a buffer layer between materials of mismatched lattice size in order to facilitate epitaxial growth.

Buffer Layer/ Insulating Layer: The buffer layer is chosen not only for suitable lattice characteristics but is also chosen based on its material properties, such as its ability to stop the chemical reactivity between ferrite and superconducting films. MgO was selected due to its low growth temperature and low dielectric constant. The low dielectric constant means that there will be little loss in the device due to its presence. The low growth temperature allows the MgO to be grown on unstable materials, such as GaAs which disintegrates for temperatures higher than 450°C. A disadvantage to the MgO is that it must be grown at a low growth pressure which adds difficulties and lengthens pumping times during the growth process. This buffer layer is anticipated to allow integration of the phase shifter with semiconductor electronics at a later phase of the project.

2. Experimental Procedures

2.1 Thin Film Growth

All of the thin films of the materials studied in this project were grown using the technique of laser ablation of the appropriate target materials in an oxygen atmosphere. The beam from a Nd:YAG laser operating at its fundamental frequency (1064 nm) was focused into the growth chamber and rastered across the target to ensure even wear of the target and a uniform plume shape. After the appropriate cleaning, the substrate was mounted on a Kanthal heater in the growth chamber. The temperature of the substrate could be maintained during growth by applying a fixed current through a heater. The growth chamber was capable of an ultimate pressure of 1×10^{-7} Torr. The oxygen pressure during ablation was controlled using a needle valve on the O₂ input line and adjusting the pumping rate in the chamber.

By varying the substrate temperature, oxygen pressure and substrate preparations conditions, the optimum growth parameters for the material in question can be determined. The parameters for the films grown in this study are listed in Table 1 below:

Table 1: Growth Parameters for Thin Film Materials

Material	Substrate Temperature (°C)	Oxygen Pressure (Torr)
YBCO	750	150×10^{-3}
MgO	350-500	5×10^{-5}
Spinel Ferrite	450-500	5×10^{-4}
Sr Hexaferrite	750	150×10^{-3}
SrRuO ₃	650	100×10^{-3}

2.2 Characterization

After growth, film thickness and refractive index could be determined using a Gaertner ellipsometer. Structural characterization was performed on a Philips PW3040 Materials Research X-ray Diffractometer, capable of 4-circle measurements. This machine is equipped with thin film optics which allowed the detection of x-ray reflections from very small volumes of material, and enabled the structural quality of the films to be determined with high accuracy.

Resistance measurements were carried out using the traditional four probe technique over temperatures ranging from 77 K to room temperature. Magnetization measurements could be done from 10K to room temperature using a Princeton Measurements Corporation Micromag alternating gradient magnetometer, which is sensitive to magnetic moments as small as 1 nanoemu.

3. RESULTS: Growth and Characterization of Device Structures

3.1 YBCO Films on Single Crystal YIG

In thin film growth, a poor in-plane lattice match does not necessarily preclude the growth of epitaxial films. Thus, despite the mismatch, it was determined to attempt first to grow high temperature superconducting YBCO films on epi-polished, single crystal YIG substrates, obtained from Deltronics, Inc. Although grown under optimum growth conditions, polycrystalline YBCO films resulted, as can be clearly seen in the x-ray scan in Figure 1. A large number of weak YBCO reflections are present in addition to the YIG substrate reflections. Resistivity measurements on these YBCO thin films showed these films to exhibit semiconducting rather than superconducting behavior, possibly indicating a chemical interaction between film and substrate, degrading the YBCO. These measurements thus show that making the device will not be simple, and that in order to deposit YBCO on YIG will require the development of suitable buffer layers.

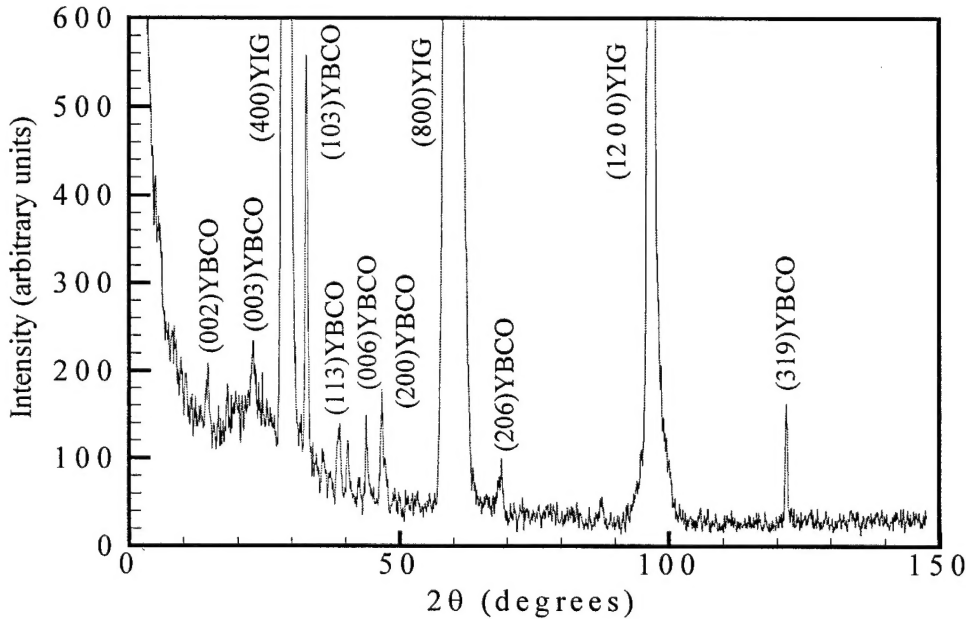


Figure 1. X-ray $\theta/2\theta$ scan of YBCO thin films grown on single crystal YIG substrates. The films are polycrystalline with semiconducting resistance.

Development of Buffer Layers

3.2 MgO Films on Single Crystal YIG

As stated in section 1.1, MgO was chosen as a buffer layer for a number of reasons. Firstly, it is known that high quality YBCO can be grown by laser ablation on single crystal MgO substrates. Secondly, MgO is insulating with a low dielectric constant, meaning that the presence of this buffer layer should not contribute to significant loss in the phase shifter. Thirdly, MgO has a lattice parameter of 4.213\AA , providing a lattice

match of approximately 1:3 with the YIG substrate. These, in combination, suggest that it should be possible to grow single crystal MgO films on single crystal YIG substrates, and subsequently grow single crystal YBCO on MgO with good superconducting properties allowing an epitaxial YBCO/MgO/YIG heterostructure to be grown.

MgO thin films were grown on polished single crystal YIG substrates to a final thickness of approximately 1000Å. X-ray $\theta/2\theta$ scans (Figure 2(a)) show only (h00) type MgO reflections in addition to the YIG substrate reflections, suggesting that the MgO films are textured, with the cubic axis lying in plane. To examine the in-plane orientation in order to determine whether the films are epitaxial, it is necessary to do x-ray pole figure measurements. Pole figure measurements allow the position of x-ray reflections from planes which are not parallel to the surface of the sample to be studied. By tilting the film from 0 to 90 degrees out of the diffraction plane while simultaneously rotating it through 360° about the surface normal, a map of the positions of normals to planes with d-spacings close to that determined by the fixed 2θ is obtained.

Figure 2(b) shows a pole figure of the (220) reflections of MgO, measured at a fixed 2θ angle of 62.3°. In this figure, the tilt angle, ψ , increases linearly along the radius of the circle, with the concentric circles marking ψ angles of 30, 60 and 90°. The rotation angle, ϕ , of the film about its normal varies tangentially from 0 to 360°. Spots of high intensity are seen from both film and substrate reflections, labeled M and S respectively. If the film were random in plane a continuous ring of reflections would be seen at $\psi=45^\circ$ rather than distinct spots, thus the pole figure shows that the film is epitaxial. However, in an ideal single crystal arrangement only four MgO {220} reflections would be present rather than the eight that are seen in Figure 2(b). This suggests that two separate in-plane growth orientations are present. From the relative positions of MgO and YIG reflections, the in-plane orientation of the film relative to the substrate can be determined as shown in Figure 2(c): the MgO cubes have grown with their in-plane axes twisted by approximately fifteen degrees from the YIG axes in plane. This growth orientation is twofold degenerate, for the MgO crystallites can nucleate with a twist either clockwise or counterclockwise from the YIG crystal, explaining the separation of thirty degrees in plane between the corresponding (220) MgO reflections seen in Figure 2(b). This fifteen degree twist can be at least partially explained from lattice mismatch conditions. A 3:1 MgO:YIG match would give 12.64Å:12.38Å in-plane match, while a twist of 15° gives a match of $3\cos 15:1$ of 12.21Å:12.38Å, a reduction of mismatch from 2.1 to 1.4%. A twist of 11.6° would give a perfect lattice match, but is likely not favored due to energy considerations of MgO atoms sitting on the YIG surface.

3.3 MgO Films on polycrystalline YIG

Single crystals of YIG proved to be difficult to obtain, as well as costly. Therefore, it was decided to attempt the growth of MgO on polished substrates of polycrystalline YIG. It was known that reasonably good epitaxy of YBCO could be attained on pressed

polycrystal MgO which had been subsequently epi-polished. If it proved possible to grow highly textured MgO films on the polycrystalline YIG, it was expected that good

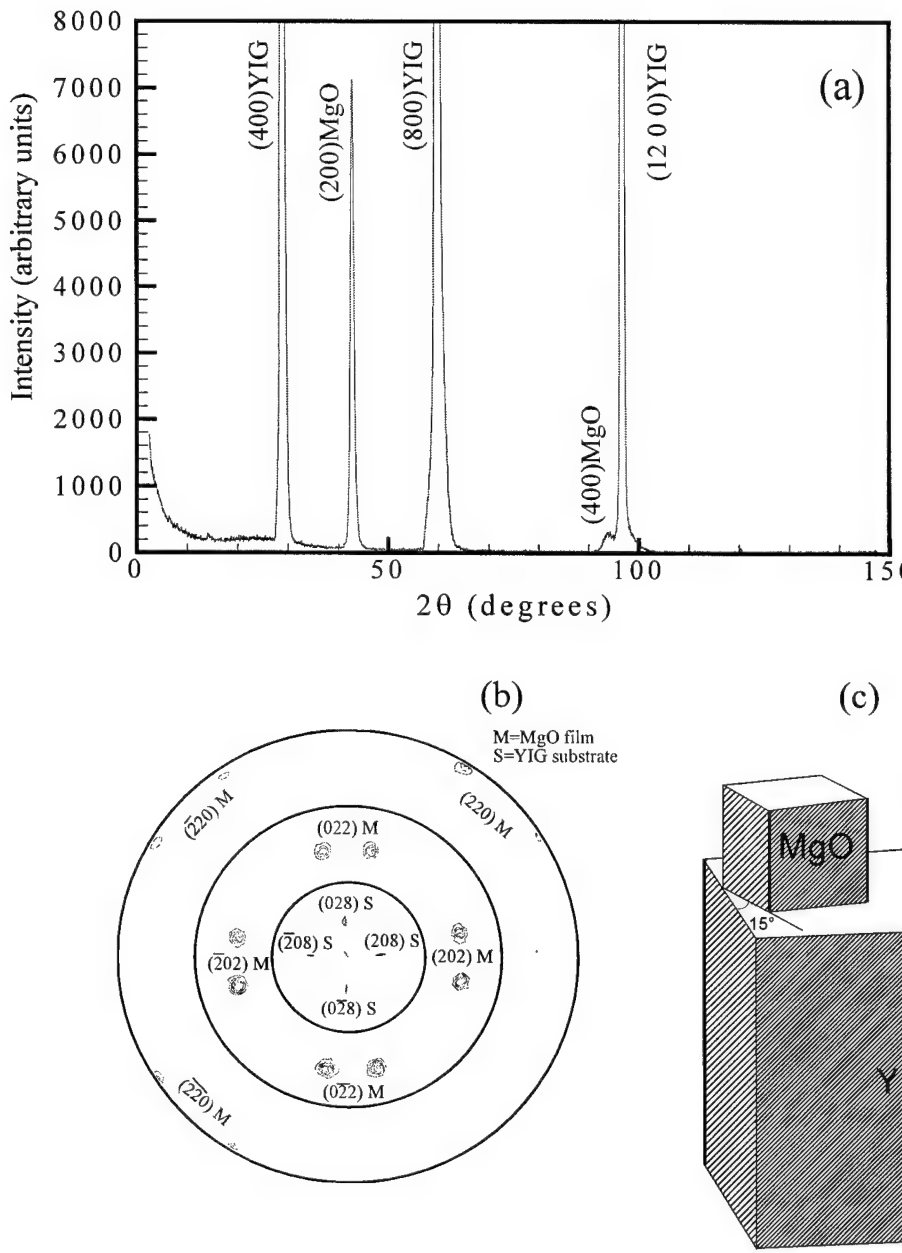


Figure 2: (a) $\theta/2\theta$ scan showing that the MgO film has grown completely (100) oriented on the YIG substrate. (b) Pole figure of the MgO (220) reflections measured at a fixed 2θ angle of 62.3° . The presence of 8 spots at $\psi=45^\circ$ indicates the presence of two growth orientations, twisted 30° from each other in plane, as shown in (c).

quality high temperature superconducting films could be grown on top of these MgO buffer layers. The YIG was polished professionally by Commercial Crystal Laboratories to an optical polish to aid smooth growth. Figure 3 shows a $\theta/2\theta$ scan for a film of MgO grown on the polished YIG. Clearly the MgO does not grow well. Only one, extremely weak MgO peak can be seen amidst the YIG reflections, while a large broad peak at 30° indicates the

presence of a large amount of amorphous MgO. Clearly MgO on polycrystalline YIG is not an appropriate combination for this project. This does not preclude the possibility that some other choice of buffer layer/polycrystal YIG combination could eventually be determined to supplant the use of single crystal YIG substrates.

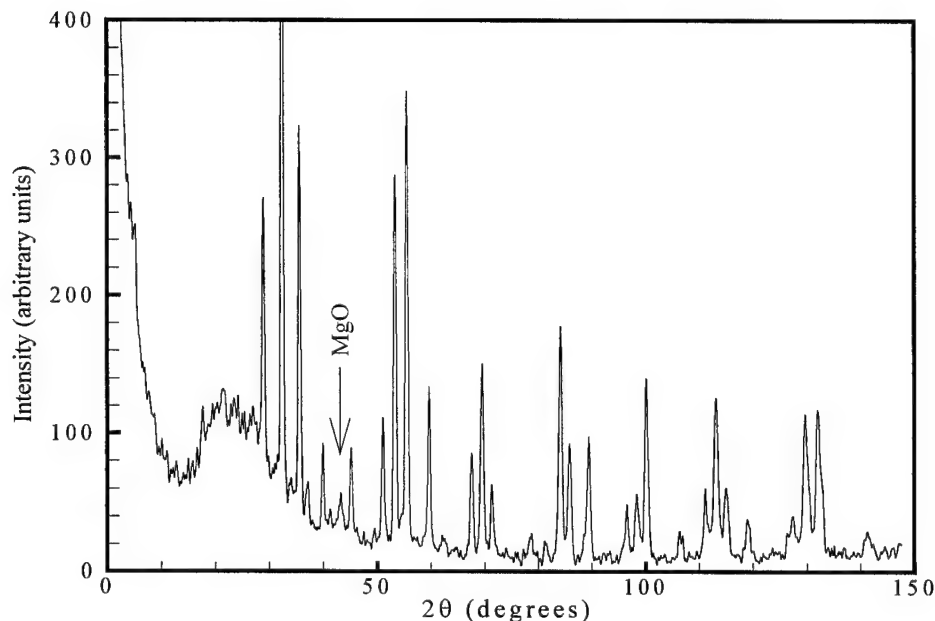


Figure 3. $\theta/2\theta$ scan of MgO grown on polished polycrystal YIG. The arrow shows the only peak attributable to MgO. Clearly MgO does not grow well on this substrate.

3.4 Investigation of MgO Buffer Layer Growth on Various Substrates

In order to optimize the characteristics of the phase shifting device, the appropriate substrate choice must be made. To assist in this, we proceeded to study the growth of our buffer layer of choice, MgO, on a wide range of single crystal substrate materials. Table 2 summarizes the results. Crystalline growth is found on cubic, hexagonal and monoclinic symmetry substrates, leading us to believe that MgO may be a surprisingly versatile buffer layer for use in many systems.

It is important to note in Table 2 that we have been able to obtain high quality single crystal films of MgO on the semiconductors silicon and gallium arsenide. This brings the devices grown on MgO closer to semiconductor fabrication, i.e., through the use of a MgO buffer layer, our materials can be integrated with semiconductor technology to produce a viable device. Both silicon and GaAs surfaces are highly reactive. In addition, at temperatures higher than 450°C, GaAs begins to break down as arsenic diffuses from the lattice, destroying the semiconducting properties and contaminating adjacent materials. For these reasons, it is hoped that a MgO buffer layer will provide not only a good lattice match but act as a chemical buffer preventing reaction with the semiconductor surface and passivating the GaAs surface.

Table 2. Growth Orientation and Epitaxy of MgO Buffer Layers

Substrate Orientation	MgO Orientation	In-plane Alignment	Lattice Mismatch
YSZ (001)	(001)	[100]MgO [100]YSZ [010]MgO [010]YSZ	2.4% for 5:4 2.4% for 5:4
YSZ (001)	(111), four orientations	[1̄10]MgO [100]YSZ [11̄2]MgO [010]YSZ	7.4% for 4:5 0.4% for 1:2
STO (001)	(001)	[100]MgO [100]STO [010]MgO [010]STO	7.9% for 1:1 7.9% for 1:1
LAO (001)	(001)	[110]MgO [100]LAO [1̄10]MgO [010]LAO	5.1% for 2:3 5.1% for 2:3
LAO (001)	(110), four orientations	[001]MgO [001]LAO [110]MgO [010]LAO	11.5% for 1:1 5.1% for 2:3
YIG (001)	(001), two orientations	15° twist in-plane of <001>	1.4% for 3:1
Si (001)	(001)	[100]MgO [100]Si [010]MgO [010]Si	3.4% for 4:3 3.4% for 4:3
GaAs (001)	(001)	[100]MgO [100]GaAs [010]MgO [010]GaAs	0.6% for 4:3 0.6% for 4:3
M-plane Al_2O_3 (10̄10)	(110)	[1̄10]MgO [001] Al_2O_3 [001]MgO [010] Al_2O_3	8.3% for 2:1 6.2% for 6:5
A-plane Al_2O_3 (1̄120)	(111) twinned	[11̄2]MgO [001̄] Al_2O_3 [1̄10]MgO [1̄10] Al_2O_3	0.7% for 5:4 1.1% for 7:5
C-plane Al_2O_3 (0001)	(111) twinned	[1̄01]MgO [100] Al_2O_3 [1̄21]MgO [120] Al_2O_3	0.7% for 4:5 0.2% for 4:5
R-plane Al_2O_3 (1̄102)	(100)	[010]MgO [1̄11] Al_2O_3 [100]MgO [110] Al_2O_3	4.2% for 7:2 6.2% for 6:5
Mica(001)	(111)	[11̄2]MgO [010]Mica [1̄10]MgO [100]Mica	0.8% for 1:2 0.7% for 3:2
GGG (111)	(111)	random in plane	1.6% for 3:1
BaF ₂ (111)	(111)	random in plane	1.6% for 3:2

Growth of Superconductor on Buffered Ferrites**3.5 YBCO Films on MgO buffered LaAlO₃**

In order to determine whether MgO buffer layers are of sufficiently high quality to allow the growth of epitaxial YBCO films, it was determined to grow YBCO first on the highest possible quality MgO films- those grown on LaAlO₃ (LAO) substrates. LAO is a common substrate used for YBCO growth, and we have found that MgO films can be grown in single crystal form on the LAO substrates. Films of YBCO on these MgO films are also of high

quality, as can be seen in the x-ray scans shown in Figures 4(a) and 4(b). Primarily c-axis growth of the orthorhombic YBCO is seen in Figure 4(a), while figure 4(b) shows that the YBCO films are aligned well with the MgO buffer layer in-plane, $[100]\text{YBCO}||[001]\text{MgO}$. The presence of very low intensity rings in the pole figure as well as the high

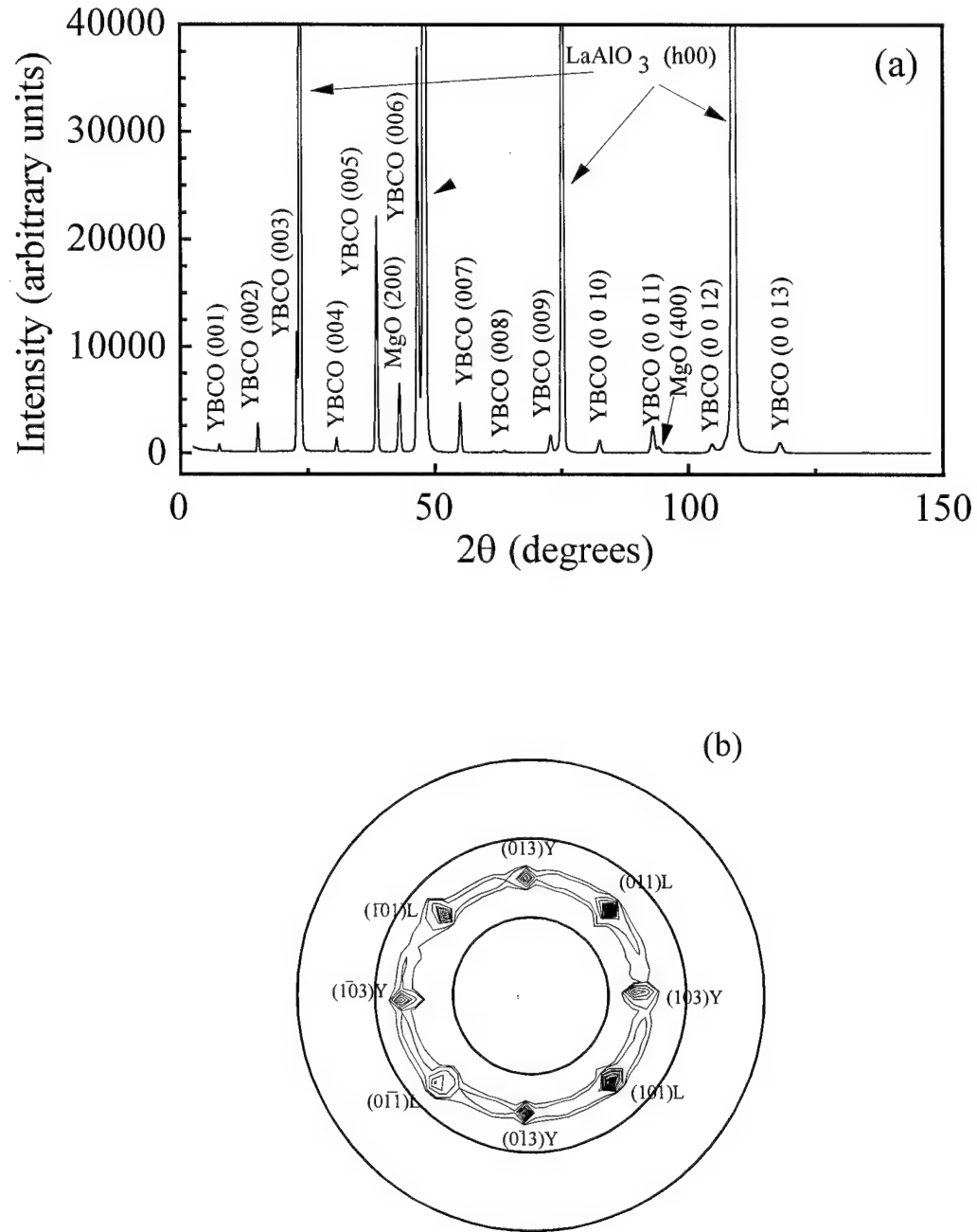


Figure 4: (a) X-ray $\theta/2\theta$ scan of YBCO grown on MgO buffered LaAlO₃, showing well-oriented YBCO growth. (b) Pole figure of the (103) poles of YBCO showing essentially single crystal growth with a slight tendency to random in plane growth shown by the weak intensity rings.

intensity spots indicates that a small amount of random in plane growth is present. Resistivity measurements (Figure 5) show very good superconducting films, with a sharp superconducting transition at $T_c=87\text{K}$. This makes us confident that MgO buffer layers can be used in layered YBCO devices, providing that the MgO can be grown of sufficient quality on the ferrite substrate (YIG or Fe_3O_4).

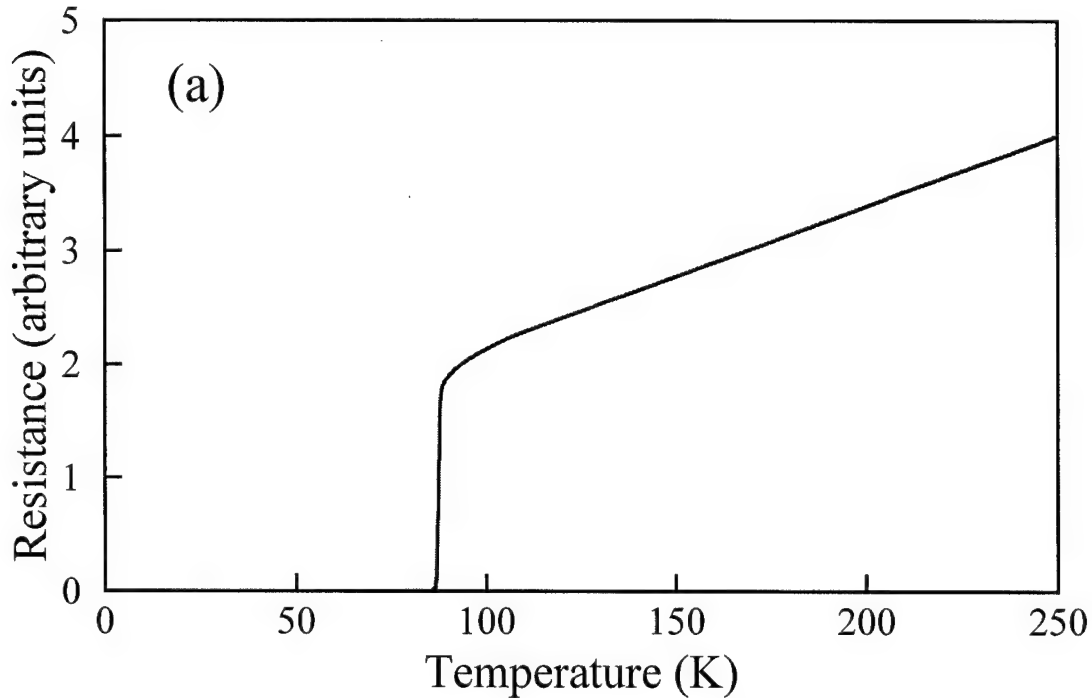


Figure 5: Resistance as a function of Temperature for YBCO/MgO/LAO. A sharp transition to the superconducting state occurs with a transition temperature of approximately 87 K.

3.6 YBCO Films on MgO buffered YIG

Our next step was to attempt to grow YBCO on the MgO films grown on single crystal YIG substrates. As described previously (Section 3.2), MgO films are epitaxial on YIG, however two different crystallite orientations are present. This may affect the quality of the YBCO films grown on the MgO buffer layer. Figures 6(a) and (b) show the x-ray measurements for YBCO/MgO/YIG samples. The YBCO has some tendency towards polycrystalline growth, as evidenced by the presence of reflections from the (103) and (130) YBCO reflections in addition to the normal (001) type growth. (103) and (130) are the highest intensity reflections in YBCO due to their multiplicity, and thus these are the reflections most likely to show non-negligible intensity with any tendency of the film towards polycrystalline growth. The in-plane orientation of the YBCO is excellent, however, as is clear in figure 6(b). Only well defined spots are present in the pole figure, showing no random in plane growth. As for the MgO/YIG in Section 3.2, the YBCO shows 8 spots rather than the expected 4, indicating that 2 sets of crystallites have grown, again rotated 30° relative to each other in plane. Thus the

YBCO nucleates with an in-plane arrangement identical to that of the MgO buffer layer underneath, causing the presence of two fold growth orientations.

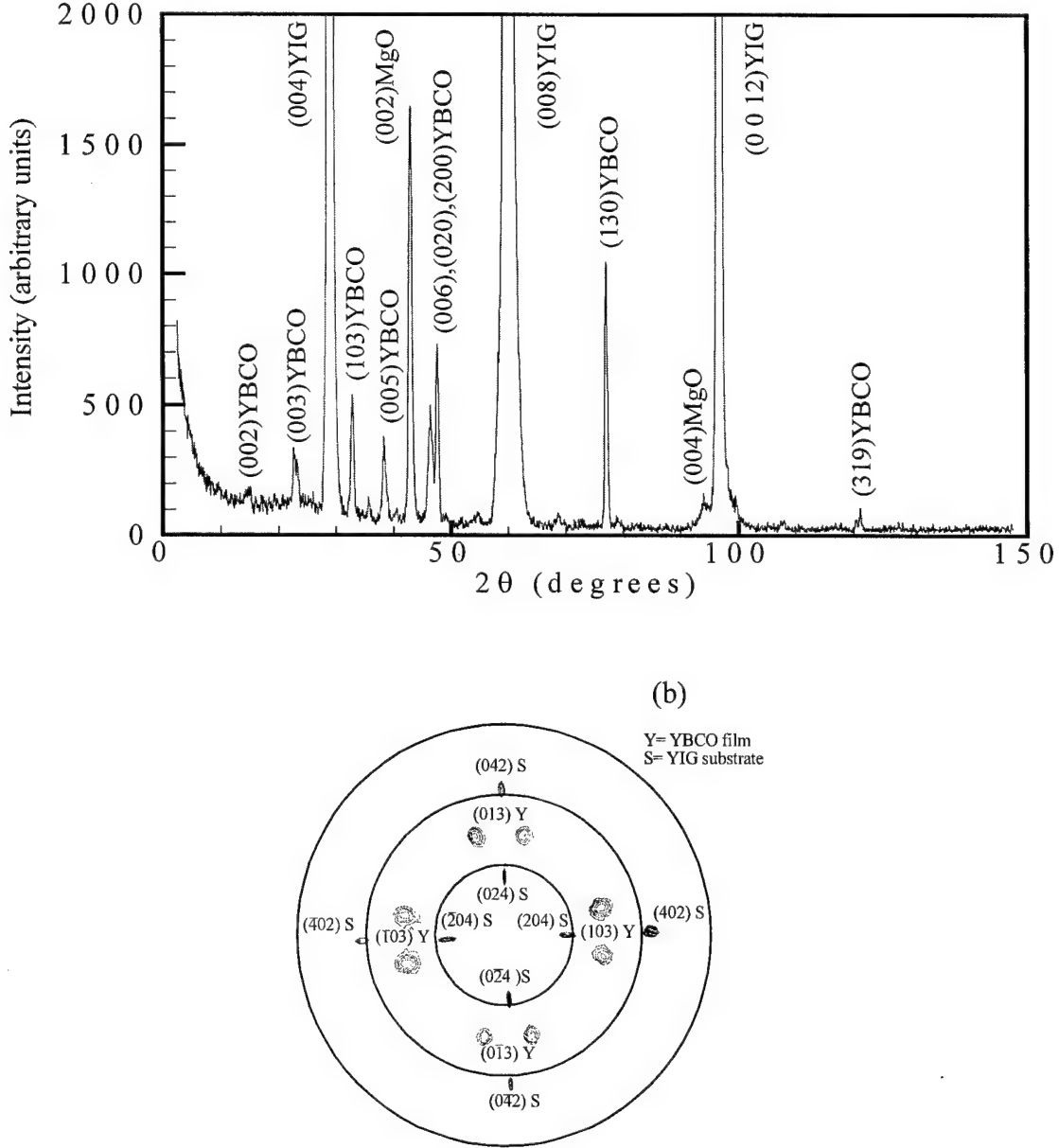


Figure 6: (a) $\theta/2\theta$ scan showing primarily (001) oriented growth of YBCO on MgO buffered YIG. The presence of (103) and (13) reflections from the YBCO indicate a slight tendency to polycrystalline growth. (b) Pole figure showing the presence of epitaxial YBCO with two in plane growth orientations rotated 30° in plane from each other, as discussed in the text.

This multiple growth pattern could result in a reduction of the superconducting nature of the YBCO due to the formation of high angle (30°) grain boundaries between the adjacent crystallites. Such grain boundaries are known to cause a reduction in critical current density due to the formation of Josephson weak-links between grains. Measurements of resistance as

a function of temperature for these films (Figure 7) reveal even further difficulties. The resistance of the YBCO at high temperatures ($>100\text{K}$), instead of increasing linearly with temperature as in figure 5, is relatively flat, with a low broad peak near 150K. This indicates that the YBCO is slightly semiconducting rather than metallic. As well, the superconducting transition, although present is severely depressed in temperature, with the YBCO being not fully superconducting down to 77K, the operating temperature of our proposed device.

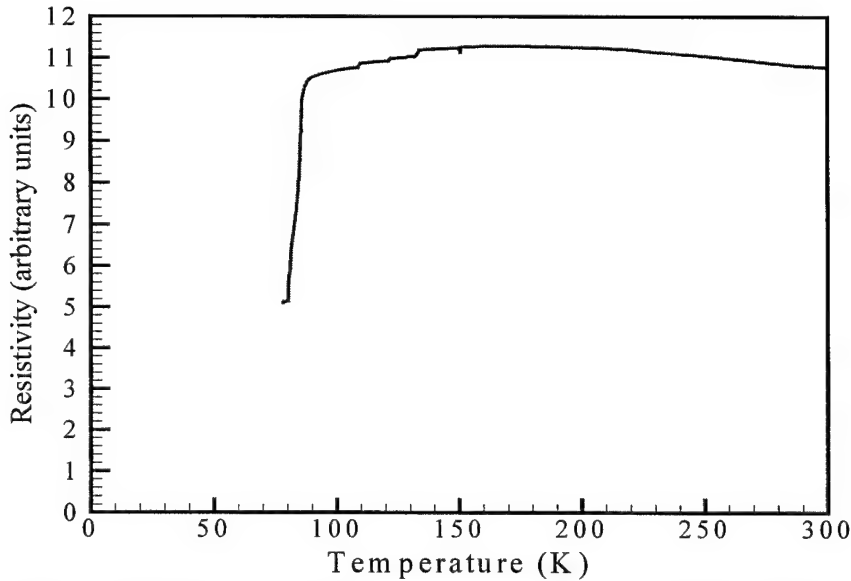


Figure 7: Resistance as a function of temperature for YBCO on MgO buffered YIG.

The suppression of T_c coupled with the semiconducting characteristics of the resistance suggests that the YBCO is slightly oxygen deficient. Since these films were grown under identical conditions to the high quality films on LaAlO_3 the decreased performance of the YBCO is most likely the result of a chemical reaction. Since the YBCO does not interact with the MgO buffer layers on LAO nor when grown on MgO substrates, the possibility arises that the YBCO is interacting with the YIG substrate, potentially forming impurity compounds such as iron or yttrium oxides, with deleterious effects on the superconducting properties. These impurities could be present to as much as one percent without being visible in the x-ray measurements, particularly if they are amorphous rather than crystalline. This suggests that either the MgO is not a sufficient buffer layer to prevent interactions or perhaps, more likely, that chemical interactions are taking place by diffusion through the multiple grain boundaries which are present in the MgO film due to the two-fold orientations. Scanning electron microscope images (Figure 8) of the surface of these films confirms the presence of many small grains with an average dimension of $1\text{ }\mu\text{m}$. It is thus necessary to find another buffer layer material which can grow epitaxially on the single crystal YIG or to concentrate on other choices of single crystal ferrite materials such as spinel or hexaferrites which can be grown in single crystal form by laser ablation.

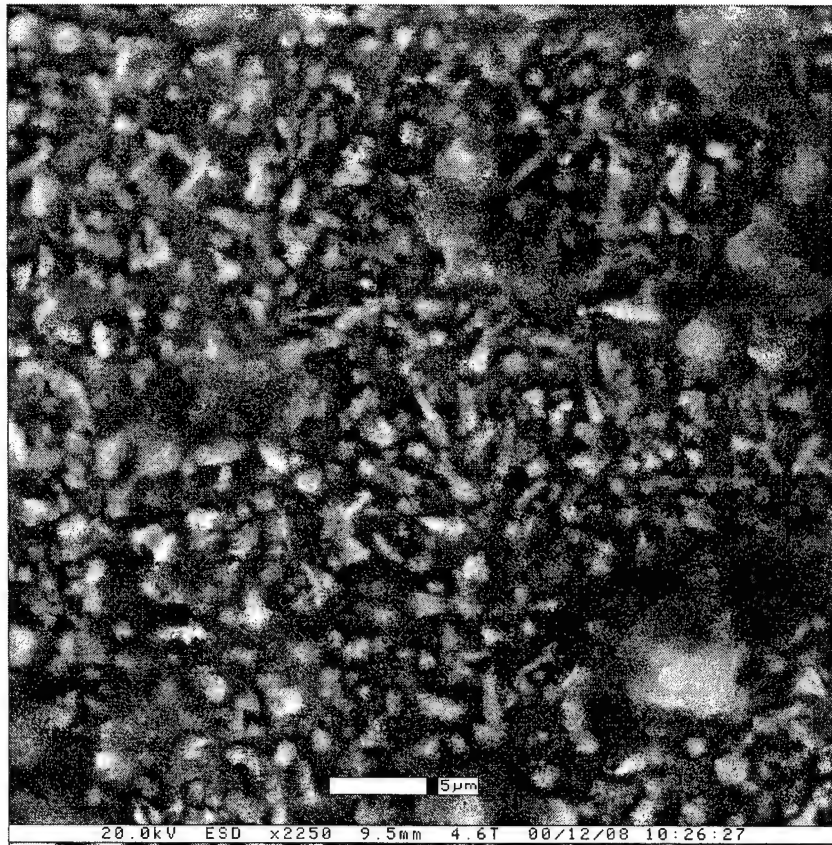


Figure 8. Scanning electron microscope image of the surface of YBCO grown on MgO buffered YIG. The presence of multiple small grains is likely a consequence of the nucleation of the MgO buffer layer in two crystallite orientations.

Growth of Ferrites

3.7 Spinel Ferrite Films on Various Substrates

Spinel ferrites such as lithium Ferrite and magnesium manganese ferrites are also suitable for use in phase shifting devices. To incorporate thick films of these materials into devices, it is necessary to be able to grow epitaxial films of YBCO and possibly buffer layers on top of films of these materials. Thus it is important to choose substrate materials on which the ferrite material will grow epitaxially. As well, since the material is in film form, the magnetic properties must also be investigated in order to determine the effects, if any, of substrate match or chemical interactions between the ferrite and the substrate materials.

Thin and thick films of various ferrites have been grown. Since most spinel ferrites have similar lattice parameters, the choice of substrate material was made by growing lithium ferrite (supplied by John Derov, Rome AF base) on a range of substrates. These results appear to generalize to a number of spinel ferrites. Table 3 lists the crystalline and magnetic properties of lithium ferrite films grown on a range of single crystal substrates and MgO buffered substrates. The spinel ferrites, with a lattice parameter close to 8.4Å, provide an

almost perfect 1:2 match with MgO (4.2Å) suggesting that, again, MgO is a potential buffer layer material. Good quality ferrite films were grown on both MgO buffered Si and MgO buffered GaAs, while films on bare Si and GaAs were polycrystalline. Thus MgO is a suitable buffer layer for use in integrating spinel ferrites with semiconductors. In general the ferrite goes down with a slight distortion from cubic due to the in-plane lattice strain, which vanishes for the thicker films (~1.1μ). The magnetization is in general larger than the expected value of 245 emu/cc, with the thicker films having values closer to the bulk value than the thinner films. Ferromagnetic resonance measurements were done on the thickest Li Ferrite samples by Dr. Carl Patton's group at Colorado State University, Fort Collins, CO. The measurements showed broad linewidths for all three thick films on SrTiO₃, YSZ and LaAlO₃ substrates. Only the film on SrTiO₃ had a measurable linewidth of 1.2 kOe, peak to peak, considerably larger than that observed in the bulk ferrite.

Table 3: Crystallographic and Magnetic Properties of Lithium Ferrite Films

Substrate	Film Orientation	In-plane Orientation	lattice mismatch	Thickness (Å)	a (Å)	b (Å)	c (Å)	M (emu/cc)	M _⊥ (emu/cc)	H _{c,} (Oe)
SrTiO ₃ (001)	(001)	[100]F [100]S [010]F [010]S	7.4% for 1:2	1700 10800	8.29 8.37	8.33 8.46	8.32 8.45	358 313	372 294	165 195
MgO/Si (001)	(001)	[100]F [100]S [010]F [010]S	-0.3% for 1:2	1700	8.409	8.401	8.424	325	300	138
MgO/GaAs (001)	(001)	[100]F [100]S [010]F [010]S	-0.3% for 1:2	1700	8.44	8.35	8.41	368	355	378
YSZ (001)	(111), twinned	[1 10]F [010]S [1 1 2]F [1 00]S	13.5% for 1:2 -0.1% for 1:4	1700 10800	8.406	8.404	8.38	349	347	107
GGG(111)	(111), 4 crystallites	<1 10>F <1 32>S	2.6% for 4:1	1700	8.51	8.38	8.49	300	286	198
Al ₂ O ₃ (001)	(111), twinned	[1 01]F [100]S [1 2 1]F [120]S	-1.5% for 2:5 -0.1% for 2:5	1700	8.41	8.40	8.38	304	293	137
Al ₂ O ₃ (110)	(111), twinned	[1 1 2]F [00 1]S [1 10]F [1 10]S	-5.0% for 3:5 -0.9% for 7:10	1700	8.4	8.6	8.4	337	329	119
Al ₂ O ₃ (100)	(100) at 30° 4 crystallites	complicated	complex	1700	-----	-----	-----	450	440	149
LaAlO ₃ (001)	(111) and (110)	random in plane	-----	1700	-----	-----	-----	428	426	144
YIG (001)	(001)	random in plane	-----	1700	-----	-----	-----	-----	-----	-----
YAG (111)	(111)	random in plane	-----	3600	-----	-----	-----	266	260	133
glass	polycrystal	random in plane	-----	1700 10800	-----	-----	-----	230 208	230 208	103 145
Si (001)	polycrystal	-----	-----	720 3600	-----	-----	-----	2498	396	185
GaAs (001)	polycrystal	-----	-----	1700	-----	-----	-----	396	376	181
LLC (111)	amorphous	-----	-----	1700	-----	-----	-----	---	---	---

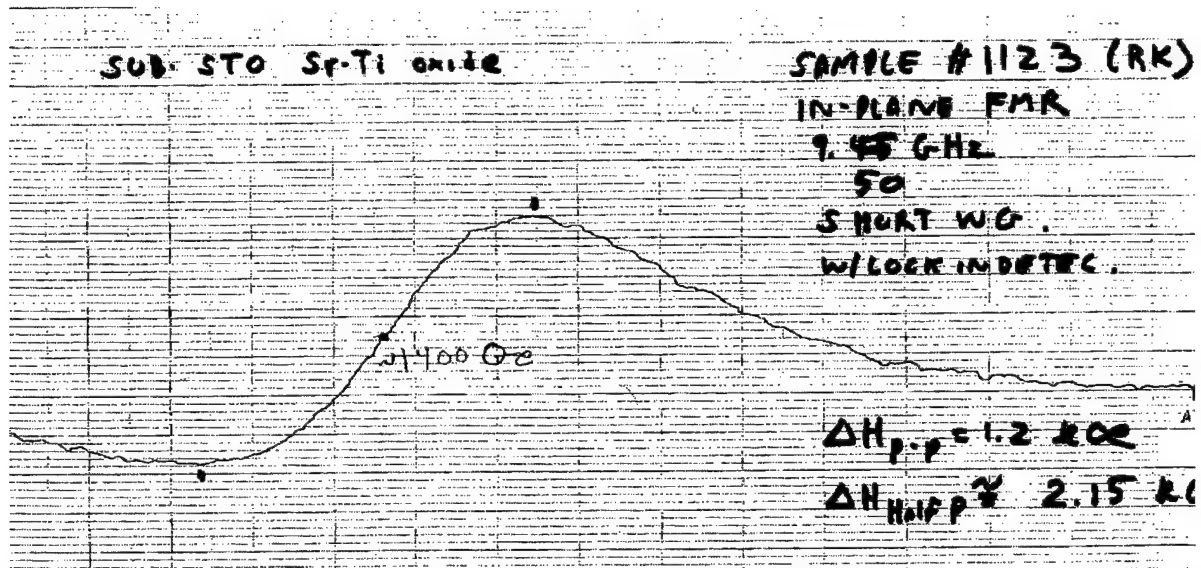


Figure 9: FMR Linewidth Measurements for the $1.1\mu\text{m}$ thick Li Ferrite film on SrTiO_3 .

It has been generally noted that spinel ferrite films grown by laser ablation often exhibit non-equilibrium properties, such as high or low magnetization, high coercivity and increased linewidth, which can be removed by a suitable heat treatment. Hour long anneals were done on a thick Li ferrite film grown on YSZ. The YSZ substrate was chosen for this test since cubic zirconia is known to be stable to high temperature, and thus should not react with the ferrite film. Figure 10 shows the results of this treatment. Clearly there is a sharp drop in coercivity with increased annealing temperature, indicating improved crystallinity. S^* , the ratio of the remanent magnetization to the saturation magnetization is used as an indication of the suitability of the magnetic material for phase shifting applications. The closer S^* (the squareness) is to one, the better the material. Annealing causes an initial rapid increase in S^* followed by a drop off with increasing temperature. Obviously annealing at an appropriate temperature, 700°C does improve the ferrite. With increased annealing temperature however comes an attendant drop in the magnetization towards zero. This may indicate the spontaneous desorption of lithium from the ferrite, a problem known to plague this particular material. Measuring the lithium concentration is difficult due to its light mass and thus decreased x-ray signal. The removal of lithium creates vacancies in the structure and a Fe_2O_3 (antiferromagnetic) like $\text{Fe}:\text{O}$ ratio will cause a reduction in film magnetization. Higher temperature anneals may be suitable for more stable spinel ferrites.

Pure Fe_3O_4 films were also grown successfully on a number of the same substrates yielding films of the same orientation as found in lithium ferrite, leading us to believe that these results can be generalized for most spinel ferrites having a cubic lattice parameter of approximately 8.4\AA .

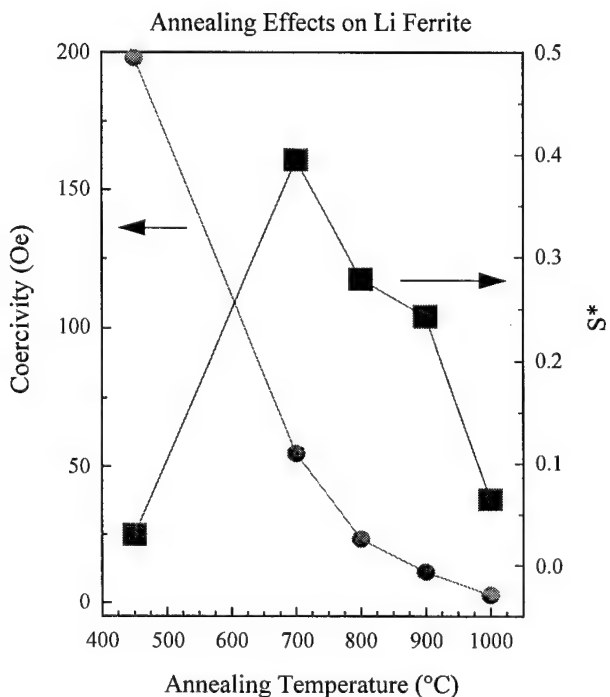


Figure 10: Effects of Annealing on the Magnetic Properties of Lithium Ferrite Films on YSZ

We conclude that there are a number of substrates such as SrTiO_3 , MgO and YSZ and various orientation of sapphire which can be used to produce high quality epitaxial films of spinel ferrites. This can allow us to tailor the substrate material to meet the demands of the final device.

3.8 Strontium Hexaferrite Films on LaAlO_3

Barium and Strontium hexaferrite materials are commonly used in phase shifting devices. In fact, thick films of hexaferrite have been made, peeled from their substrates and incorporated in phase shifters by other research groups. This, however, leaves the problem of an “air gap” between the materials leading to loss of signal. In order to improve performance, it is necessary to grow these bulk films directly on the substrate of choice, or on a suitable buffer layer in the layered device. Hexagonal ferrites are formed by layers of cubic garnet stacked along their (111) cube diagonals (thus the hexagonal symmetry) with intervening BaO or SrO layers. The cubic building blocks leads us to believe that it may be possible to grow these films on cubic substrates, or indeed on our cubic MgO buffer layers.

To initiate our study, we chose to grow films on single crystal LaAlO_3 (LAO) substrates, as they are relatively inexpensive, and have a similar lattice parameter to MgO . Growth of Sr Hexaferrite (SRM) on these films resulted in two prevailing growth orientations—the films nucleate either with their c-axis (hexagonal axis) perpendicular to the substrate surface or at a 55° angle to the plane. Variations of growth conditions failed to result in the discovery of

conditions under which either of these orientations could be selectively grown. Only by x-ray measurements after growth could these two orientations be distinguished.

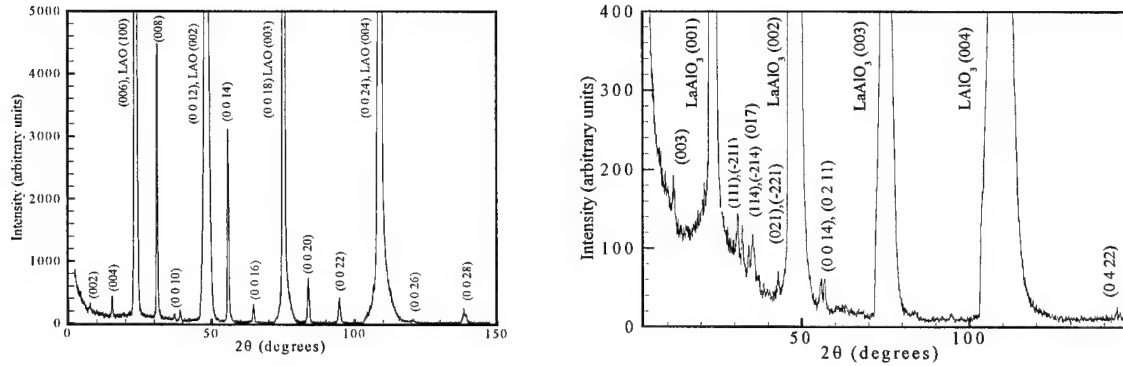


Figure 11: Comparison of the X-ray $\theta/2\theta$ scans for c-axis oriented growth (left) and growth with the c-axis at 55° to the plane (right). In the latter case, no large peaks occur in the x-ray scan, leading one to believe, erroneously, that the film is polycrystalline and of low quality.

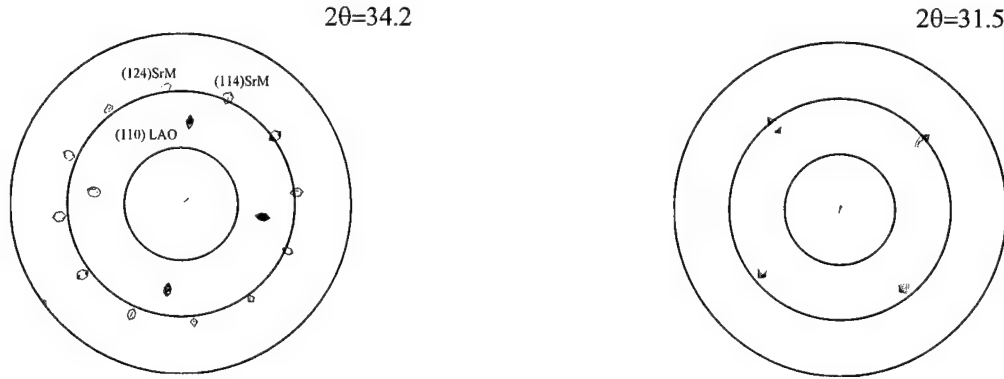


Figure 12: (left) Pole figure of the c-axis oriented SRM films. The position of the SRM reflections indicate that the SRM is epitaxial, with four crystallites present, rotated 90° from each other in plane due to the four fold symmetry of the LAO substrate. (right) Pole figure showing the position of the c-axis reflections for the second growth orientation of SRM. These spots are at 55° to the substrate normal. Again four unique growth orientations are present. In a single crystal one would see only a single reflection at 55° .

The nucleation of SRM crystallites with their c-axes inclined at 55° to the substrate surface can be easily understood when the underlying geometry of the material is examined. As stated above, the SRM c-axis is coincident with the (111) cubic axis of the garnet building blocks. The angle between (111) and (100) planes in a cubic material is 54.7° suggesting that the SRM has grown such that the (111) planes of the garnet layers are aligned with the (111) planes of the underlying (100) oriented LAO substrate. This is further corroborated by the presence of four such growth orientations, twisted 90° from each other in plane, so as to force the $\langle 100 \rangle$ directions in the cubic garnet to align with the four-fold $\langle 100 \rangle$ directions of the LAO substrate in plane. This suggests that it should be possible to grow single crystal SRM

films on a cubic substrate if that substrate is (111) oriented and has the appropriate lattice parameter match.

The obvious choice for a substrate is MgO, however (111) oriented MgO single crystals are difficult to impossible to obtain due to the difficulty of polishing the substrate without causing severe distortion along the cleavage directions. The next possibility is to examine thin films of MgO: if (111) oriented single crystal thin films could be produced, they could be very valuable for this project. However, only one substrate was found to produce single crystalline (111) oriented MgO, namely mica (see Table 2). Unfortunately, mica can not be subjected to the high growth temperatures of 750 °C necessary for the subsequent epitaxial growth of SRM and YBCO. The layers in mica begin to separate due to the breaking of the weak bonds between them at temperatures close to 600°C. (111) oriented growth was also found on sapphire, however it grew twinned, which would induce defects in the SRM film grown upon it. Thus it has not been possible to attempt the growth of SRM on (111) oriented single crystal MgO.

The magnetic properties of the SRM films were investigated via hysteresis loop measurements, shown in figure 13, below.

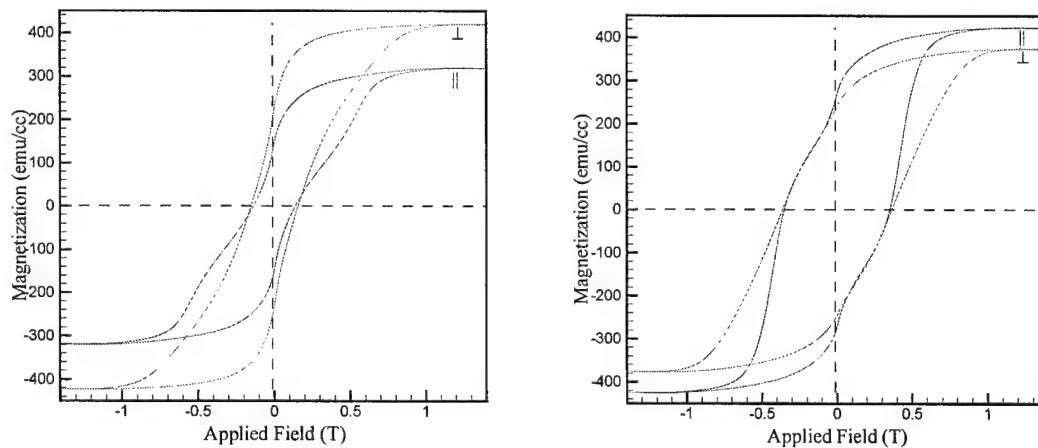


Figure 13: Magnetization of (left) c-axis oriented SRM films on LAO and (right) SRM films grown with their c-axes at 55° to the LAO surface.

The films in which the c-axis is grown at 55° to the substrate surface have a coercivity more than twice that of the c-axis oriented film, an indication of the large, symmetry induced magnetic anisotropy. The saturation magnetization has similar values for the two orientations, confirming that the chemistry of the films are the same. The squareness ratio S^* is slightly higher for the off-axis film, however the increased coercivity makes use of these films impractical since they would require extremely large latching currents to saturate the ferrite.

Semiconductor Integration

3.9 YBCO Films on MgO Buffered Semiconductors

The growth of single crystal MgO buffer layers on semiconductors has allowed us to integrate ferrite thin films with semiconductor media. It now remains to attempt growth of high temperature superconducting materials on these semiconductors. YBCO is grown at an elevated temperature of 750°C which may be expected to cause some difficulties with this growth. For silicon, difficulties arise due to the large thermal expansion coefficient of silicon relative to both MgO and YBCO. This means that the substrate will expand and shrink dramatically upon heating and cooling, potentially causing cracking and strain in both the MgO buffer layer and the YBCO film.

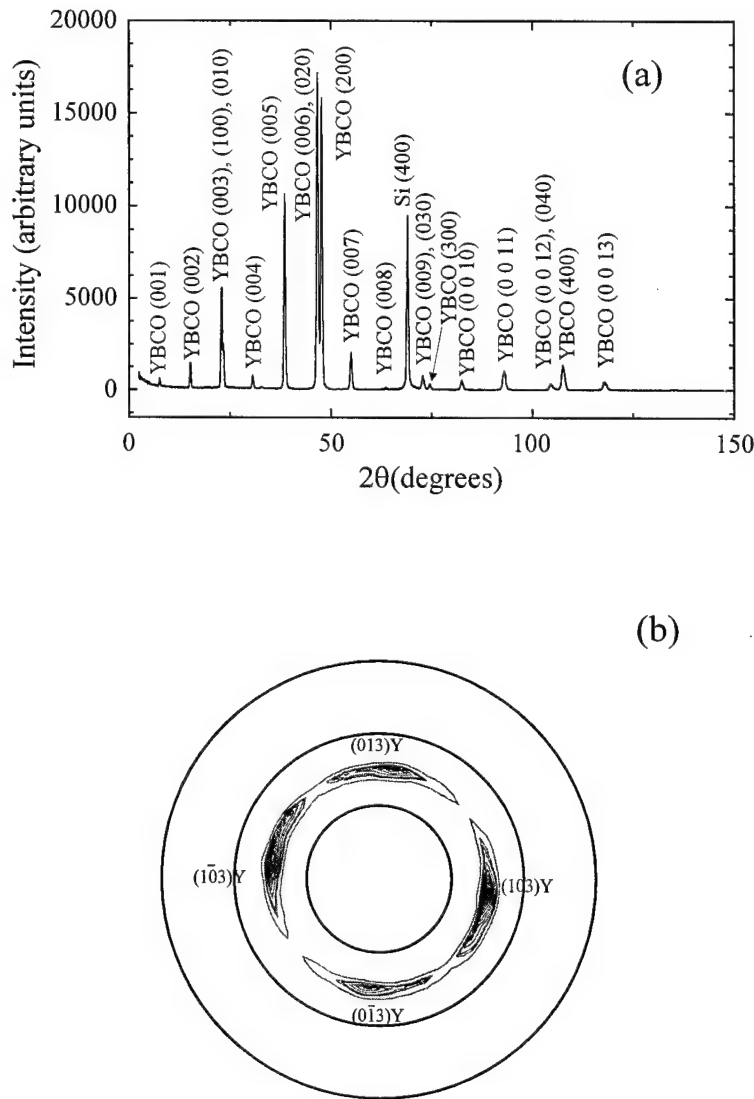


Figure 14: (a) $\theta/2\theta$ scan showing primarily (001) oriented growth of YBCO on MgO buffered Si. (b) Pole figure showing the presence of epitaxial YBCO with a tendency to random in plane growth.

Figures 14 (a) and 14(b) show the x-ray $\theta/2\theta$ and pole figure measurements, respectively, for a film of YBCO grown on silicon. The YBCO is (001) oriented with a small amount of (100) and (010) growth present. The pole figure measurements of the (103) YBCO reflections shows the presence of four rather broad spots spread out azimuthally. This is in contrast to the films grown on MgO buffered LaAlO₃, for which 4 rather sharp YBCO (103) reflections could be seen (Figure 4(b)). This spread indicates a distinct tendency towards random in-plane growth, caused perhaps by cracking of the MgO buffer layer on which the YBCO was grown due to thermally introduced strain. The presence of this strain is supported by the distinct absence of reflections from the MgO buffer layer in Figure 14(a), suggesting that the MgO crystallites have been disordered in some way. Such breakup has been documented in cases of high temperature growth of materials with dissimilar thermal expansion coefficients.

To investigate whether this reduction in epitaxy has deleterious effects on the superconducting properties, resistance measurements as a function of temperature were done (Figure 15). Clearly the YBCO is metallic at high temperature, with a sharp superconducting transition at a temperature of 85 K. The width of the superconducting transition is approximately 3K, similar to that seen in the high quality YBCO films grown on MgO buffered LaAlO₃ (Section 3.5). This indicates that although the MgO buffer layer may be cracked, there is no obvious chemical reaction taking place between the silicon substrate and the YBCO layer. We thus conclude that MgO is a reasonable buffer layer for growth of YBCO on Si. To improve epitaxy and thus the ability to use it for high quality multiple-layered devices, it may be necessary to investigate other buffer layer materials. Presumably a buffer layer which grows at temperatures similar to that for YBCO (such as CeO₂) and has a thermal expansion coefficient similar to silicon may prove less vulnerable to thermal break-up.

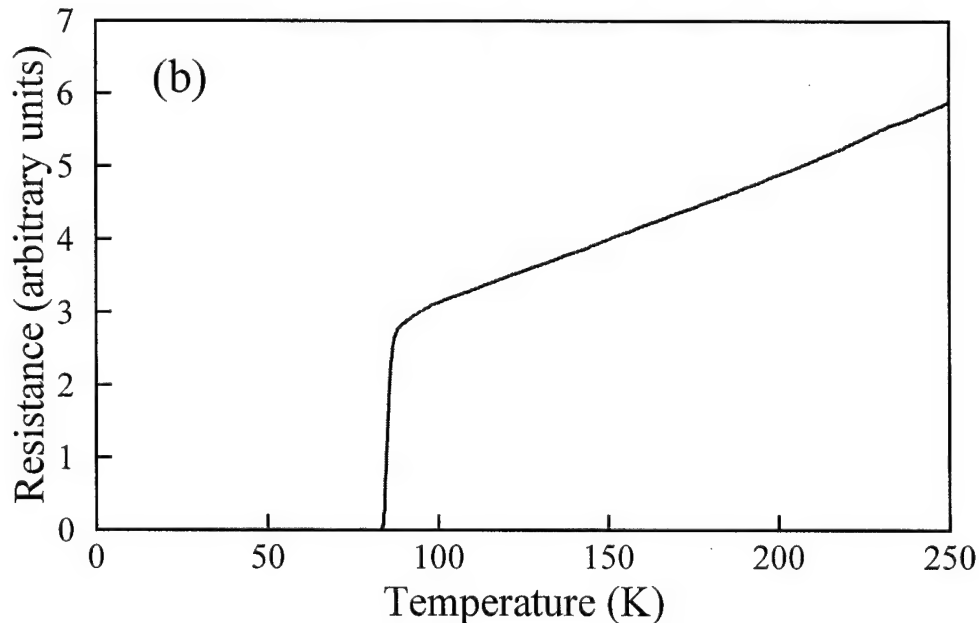


Figure 15: Temperature Dependence of the Resistance of YBCO/MgO/Si

YBCO films were also grown on MgO buffered GaAs substrates. At the elevated growth temperatures of 750°C, diffusion of arsenic from the uncoated back and sides of the GaAs

substrates occurred, both destroying the GaAs and the YBCO film on top of it. The GaAs was then ‘encapsulated’ by growing MgO films on both the front and back surfaces of the substrates (~5mm x 5mm x 0.5mm). However, diffusion from the edges still proved to be sufficient to destroy the YBCO films grown on top of the MgO buffer layer, and indeed, to contaminate the growth chamber such that thorough disassembly and cleaning was necessary before crystalline YBCO films could again be grown.

If GaAs is to be the superconducting substrate of choice, as is preferable for its good properties at r.f frequencies, it will become necessary to find some effective method of encapsulation which will allow epitaxial films to be grown and at the same time keep As from diffusing into the growth chamber. The current technology of spin-on coatings covers the surface to be deposited on. Thus it is difficult to open a via on which to grow the YBCO but may prove useful for coating the back and sides of the GaAs substrate.

Ground Plane Development

3.10 SrRuO₃ and CaRuO₃ Films on LaAlO₃

As discussed in the introduction, a functioning phase shifter needs ferrite, superconducting, and buffer layers. There is also need for a conducting ground plane. It is desirable that this metallic plane provide a good lattice match for the other layers in order to allow epitaxial growth. SrRuO₃ and CaRuO₃ are excellent choices for such a material. These are both metallic perovskites, with lattice parameters which allow extremely close match to the YBCO lattice, and are commonly used in YBCO/metal tunnel junction and multilayers. For this reason it was decided to grow these films on LaAlO₃ substrates. Since we have been able to grow YBCO, MgO and ferrites on LaAlO₃, LaAlO₃ is a good substrate on which to attempt device integration.

The ruthenate materials were grown at a variety of growth temperatures in order to ascertain the best substrate temperature-as always, we would like to keep the growth temperature as low as possible to aid in potential integration with Si and GaAs, i.e. to avoid the difficulties stated in section 3.9. It was noticed that the films developed a secondary growth orientation for substrate temperatures lower than 600°C. This secondary orientation does not seem to have an immediate effect on the bulk properties of the material, in fact, some properties improve by relieving substrate strain through grain boundary formation. Table 4 lists the structural and physical parameters of SrRuO₃. SrRuO₃ is ferromagnetic below 160K, so the effects of growth temperature on the Curie temperature as well as on the bulk resistivity was measured. In this table, a, b and c represent the lattice parameters of the standard perovskite growth, while a', b' and c' indicate the parameters of the secondary orientation, if present. Examination of Table 4 shows that the lattice strain is greatly reduced in the presence of the secondary orientation.

Figure 16 shows the overall effect of substrate temperature on the room temperature resistivity and the mosaicity (rocking curve width) of the films. Clearly, there is a fairly wide range of

temperature for which the resistivity and the mosaicity are low, suggesting that these films may be grown at reasonable low temperatures without severe degradation of the desired properties. In fact the resistivities seen even in the films with two growth orientations is similar to that observed in single crystals of SrRuO_3 , and is lower than noted in thin films grown by groups who have successfully integrated these materials with YBCO thin films. It remains to be seen however what effect the multiple orientations present at low growth temperature may have on YBCO films grown on this ground plane.

Table 4. X-ray and resistivity data for SrRuO_3 films grown on LaAlO_3 . The number in brackets indicates the uncertainty in the last digit quoted. The primed columns indicate data from the secondary orientation of SrRuO_3

Growth Temp (°C)	a (Å)	b (Å)	c (Å)	$\overline{\Delta\omega}$ (°)	a' (Å)	b' (Å)	c' (Å)	$\overline{\Delta\omega}'$ (°)	$\rho(300\text{K})$ $\mu\Omega\text{-cm}$	T_c (K)	$d\rho/dT$
760	5.544(2)	5.547(2)	7.841(2)	1.03	-----	-----	-----	-----	14,000	-----	-----
710	5.545(2)	5.550(2)	7.844(3)	1.07	-----	-----	-----	-----	3,000	155(5)	-----
670	5.548(7)	5.551(7)	7.850(9)	0.98	-----	-----	-----	-----	230	154(5)	-----
640	5.546(2)	5.548(2)	7.850(2)	0.67	5.545(4)	5.559(9)	7.861(7)	0.93	250	151(5)	-----
590	5.537(2)	5.555(2)	7.842(2)	0.78	-----	-----	-----	-----	374	148(2)	-----
535	5.534(2)	5.564(2)	7.852(3)	0.67	5.525(7)	5.56(1)	7.88(1)	0.84	482	149(2)	-----
490	5.546(2)	5.551(2)	7.852(3)	0.71	5.550(7)	5.56(2)	7.82(1)	0.80	526	154(3)	-----
445	5.538(2)	5.556(2)	7.841(3)	0.62	5.546(7)	5.55(1)	7.83(1)	1.0	285	151(3)	-----
390	5.535(2)	5.558(2)	7.850(3)	0.84	5.5(2)	5.5(2)	7.86(2)	3.0	610	149(2)	-----
340	5.536(5)	5.551(5)	7.845(4)	1.31	5.6(1)	5.5(2)	7.87(2)	2.9	1,100	147(2)	-----
340	5.534(5)	5.564(5)	7.853(7)	1.37	5.557(6)	5.54(1)	7.896(9)	3.5	1750	146(3)	-----
300	-----	-----	-----	-----	-----	-----	-----	-----	38,000	-----	-----
240	-----	-----	-----	-----	-----	-----	-----	-----	-----	-----	-----

The ferromagnetic state in the SrRuO_3 at the operation temperature of 77K may complicate analysis of the phase shifter, in which case it may be preferable to study CaRuO_3 films instead. We found that CaRuO_3 films grew over a slightly abbreviated temperature range compared to SrRuO_3 films. However no secondary growth orientations are observed in these films, perhaps due to a better lattice match of the slightly smaller CaRuO_3 cell with the LaAlO_3 lattice. The properties of these films are shown in Table 5 below. Clearly, CaRuO_3 may be a better choice than SrRuO_3 for the ground plane of a simple phase shifting device, although the ferromagnetism of SrRuO_3 might lend itself to some interesting applications.

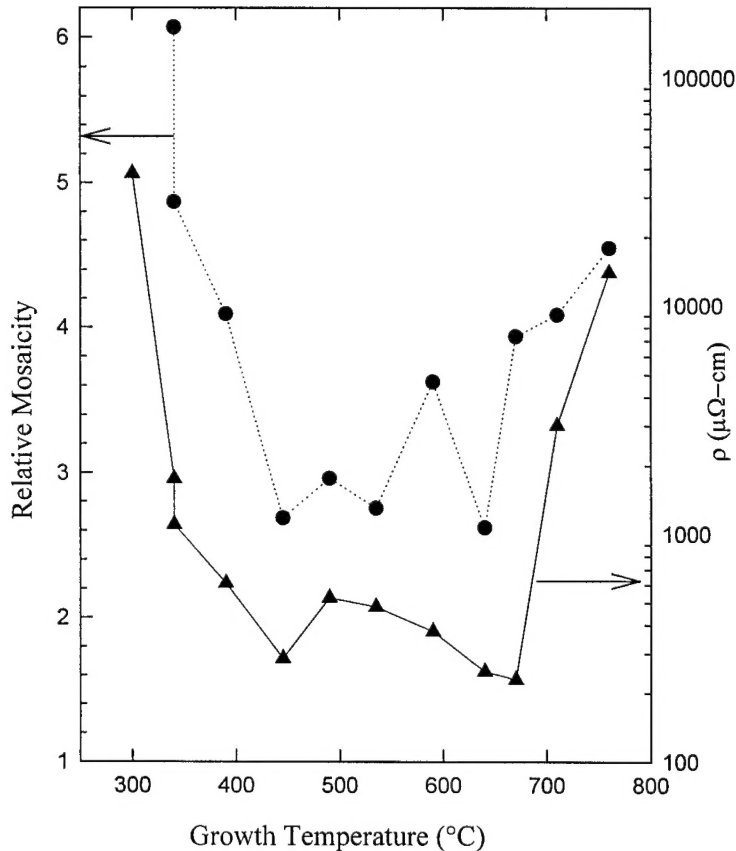


Figure 16: Dependence of the Room temperature Resistivity and Crystalline Mosaicity on Substrate Temperature During Growth.

Table 5: Properties of CaRuO_3 Thin Films on LaAlO_3

Temperature (°C)	a (Å)	b (Å)	c (Å)	V (Å ³)	$\overline{\Delta\omega}$ (°)	$\rho(300\text{K})$ $\mu\Omega\text{-cm}$
750	5.409(7)	5.425(7)	7.636(9)	224.1(5)	0.89	247
720	5.407(9)	5.418(9)	7.64(6)	223.8(6)	0.76	213
690	5.42(2)	5.37(3)	7.64(3)	222(2)	0.92	124
660	5.41(1)	5.42(1)	7.63(1)	223.7(7)	0.98	156
660	5.41(1)	5.41(1)	7.61(1)	222.8(7)	0.85	163
627	5.415(7)	5.418(7)	7.634(9)	224.0(5)	0.96	173
590	5.41(1)	5.44(1)	7.63(2)	224.3(8)	0.96	112
548	5.428(7)	5.411(7)	7.649(8)	224.7(5)	0.98	109
505	5.44(1)	5.42(1)	7.67(2)	226.5(8)	1.01	151
460	5.406(8)	5.465(8)	7.67(1)	226.6(6)	0.97	122
420	5.427(7)	5.444(7)	7.689(9)	227.2(5)	1.00	180
375	----	----	----	----	----	insulating

3.11 YBCO Thin Films on CeO₂/YSZ/Ni

Finally, to investigate further technological possibilities, YBCO films were grown on biaxially textured Ni substrates, which had been prepared for us with CeO₂/YSZ buffer layers at Oak Ridge National Laboratories. Textured Ni is not only extremely cheap, it is also flexible, lending itself to applications in high temperature superconducting 'wires' etc. X-ray scans of these films showed the presence of highly textured YBCO films, in addition to some polycrystalline orientation. The presence of these random orientations may well affect the operating conditions of the material. As well, the magnetic nature of the Ni substrate may also affect the switching of the ferrite and introduce some loss. It is interesting however to note the ability to grow epitaxial YBCO on textured metals. As well, CeO₂/YSZ has been shown to be an appropriate buffer layer for YBCO. Unfortunately these are both grown at high growth temperatures, precluding their use as an effective buffer for GaAs. They might however prove effective for silicon applications.

4. Future Directions

The intended device design was as described in Section 1. As was found during the development stages, depending on the substrate material used, buffer layers might be required between the substrate and the ground plane. Buffer layers are definitely required to allow growth of epitaxial YBCO for both the control line and the meander line. This will mean at least three layers of MgO. As well, we will be growing the top ferrite layer forming the 'toroid' on top of a YBCO layer. This requires high quality buffer layers of MgO on which the ferrite can grow almost seamlessly from the interface of ferrite on ferrite to ferrite on buffer layer.

The presence of multiple layers complicates matters, since epitaxy degrades with ferrite film thickness. The top meander line then will not have as high a quality surface on which to grow. Since the superconducting properties of the meander line are one of the most vital properties in the phase shifter, a 'bottoms up' design appears better. In this design, the YBCO would be deposited on a suitable substrate with a MgO buffer layer. The meander line would be patterned and the ferrite toroid with control wire could be grown on top. The top layer then would be the ground plane, whose properties are not critical. Even a sputtered or evaporated metallic film would be adequate. The difficulty in the 'bottoms up' design would be in patterning the YBCO meander line, and ensuring connections to this line after films are grown on top, most likely by partial masking of the substrate. These problems are not insurmountable.

Integration with semiconductors may be more difficult. Although the ferrite toroid can easily be grown on the semiconductors, the superconducting strip is not so easy due to the difficulties of high temperature processing of the semiconductors, especially GaAs. We suspect that buffer layers such as CeO₂ and/or YSZ will make for higher quality growth of YBCO on silicon than MgO buffer layers. Growth on GaAs will require much more work to find an appropriate passivation layer to prevent As desorption from the surface.

5. Students Employed

This project was hampered by our inability to hire a suitable post-doctoral fellow due to the interference of FAMU administration. This resulted in the loss of one year's funding on this grant and more importantly the absence of a set of hands to carry out the proposed work.

We did however hire a number of undergraduate students, as well as one master's level student during his transition from masters to Ph.D. student level. These students, in accordance with Florida A&M University's status as a Historically Black College (HBCU) were African American. The undergraduates (both physics and engineering majors) were employed primarily during the summer months. They assisted in various aspects of research including film growth and characterization as well as equipment manufacturing and library research into appropriate buffer layer materials and previous work in this field.

Their names are as follows:

Linea Baker
Armand Belcher
Bridgette Bell
Natanette Craig
Timothy Hogans
Jessica Jeffcoat
Gregory Triplett

6. Publications

A number of publications were completed on the material covered in this project. The complete references are listed below. Copies of these publications are enclosed.

1. Effect of Substrate Temperature on Growth of SrRuO_3 and CaRuO_3 Thin Films, R.J. Kennedy, R. Madden and P.A. Stampe. Submitted to J.Phys. D : Appl. Phys.
2. Reciprocal space Mapping of Epitaxial MgO Films on SrTiO_3 , R.J. Kennedy and P.A. Stampe, J. Crystal Growth, **207** (1999) 200.
3. Growth of MgO thin films on M-, A-, C- and R-plane sapphire by laser ablation P A Stampe, M Bullock, W P Tucker and Robin J Kennedy, J. Phys. D: Appl. Phys. (1999) **32** 1778.
4. Growth of $\text{YBa}_2\text{Cu}_3\text{O}_{7-x}$ thin films on LaAlO_3 and Si with MgO Buffer Layers, P.A. Stampe, W.P. Tucker and R.J. Kennedy, Physica C 314 (1999) 69.
5. Fe_3O_4 films grown by laser ablation on Mica with and without MgO buffer layers, R. J. Kennedy and P. A. Stampe, J. Magn. Magn. Mat. **195** (1999) 284.

6. Fe_3O_4 films grown by laser ablation on Si and GaAs substrates with and without MgO buffer layers, R. J. Kennedy and P. A. Stampe, *J. Phys. D: Appl. Phys.* **32** (1999) 16.
7. X-ray Characterization of MgO Thin Films Grown by Laser Ablation on SrTiO_3 and LaAlO_3 , P.A. Stampe and R.J. Kennedy, *J. Crystal Growth*, **191**(1998), 478.
8. X-ray Characterization of MgO Thin Films Grown by Laser Ablation on Yttria-stabilized Zirconia, P.A. Stampe and R.J. Kennedy, *J. Crystal Growth*, **191** (1998), 472.
9. Growth of MgO on Si(100) and GaAs(100) by Laser Ablation, P.A. Stampe and R.J. Kennedy, *Thin Solid Films* **326** (1998) 63.

The following papers are in preparation, pending some slight revision:

1. Structural and Magnetic Properties of Lithium Ferrite Films grown by Laser Ablation, P.A. Stampe, R.J. Kennedy, A. Srivastava and C. Patton
2. Growth of YBCO Thin Films on Single crystal YIG Substrates for Microwave Device Applications, R.J. Kennedy and P.A. Stampe.
3. Anomalous Growth of Epitaxial Strontium Hexaferrite Thin Films on LaAlO_3 , R.J. Kennedy and P.A. Stampe.
4. Characterization of NiO and Co_3O_4 Films grown on Mica, R.J. Kennedy and P.A. Stampe.

As well, the following abstracts have appeared in national proceedings:

1. Texture Analysis of MgO Thin films on Crystalline Substrates, *Bulletin of the American Physical Society*, March 1999.
2. Growth of Fe_3O_4 on Mica With and Without MgO Buffer Layers, *International Conference on Magnetism and Magnetic Materials*, Miami, Florida, November 10, 1998.
3. Why do you need a 4-circle x-ray diffractometer for thin-film analysis?, Fall Meeting of the South Eastern Section of the American Physical Society, Miami, Florida, November 13, 1998.

As well, presentations have been made at a number of program review meetings.